

Biopolymeric In Situ Hydrogels for Tissue Engineering and Bioimaging Applications

Adonijah Graham Sontyana¹ · Ansuja Pulickal Mathew¹ · Ki-Hyun Cho² · Saji Uthaman³ · In-Kyu Park¹

Received: 25 June 2018 / Revised: 20 August 2018 / Accepted: 21 August 2018 / Published online: 14 September 2018
© The Korean Tissue Engineering and Regenerative Medicine Society and Springer Science+Business Media B.V., part of Springer Nature 2018

Abstract

BACKGROUND: Biopolymeric *in situ* hydrogels play a crucial role in the regenerative repair and replacement of infected or injured tissue. They possess excellent biodegradability and biocompatibility in the biological system, however only a few biopolymeric *in situ* hydrogels have been approved clinically. Researchers have been investigating new advancements and designs to restore tissue functions and structure, and these studies involve a composite of biometrics, cells and a combination of factors that can repair or regenerate damaged tissue.

METHODS: Injectable hydrogels, cross-linking mechanisms, bioactive materials for injectable hydrogels, clinically applied injectable biopolymeric hydrogels and the bioimaging applications of hydrogels were reviewed.

RESULTS: This article reviews the different types of biopolymeric injectable hydrogels, their gelation mechanisms, tissue engineering, clinical applications and their various *in situ* imaging techniques.

CONCLUSION: The applications of bioactive injectable hydrogels and their bioimaging are a promising area in tissue engineering and regenerative medicine. There is a high demand for injectable hydrogels for *in situ* imaging.

Keywords Bioimaging · Biopolymeric injectable hydrogels · Gelation

1 Introduction

Hydrogels are hydrophilic polymer networks that can absorb large amounts of water, up to two thousand times greater than their dry weight. Hydrogels are formed by the binding of polymeric networks through hydrogen-bonding, hydrophobic forces, and secondary forces, including ionic or molecular entanglements [1, 2]. Due to molecular entrapment clusters, ionically associated domains or hydrophobicity, some hydrogels are not physically homogeneous and contain inhomogeneity. Hydrogels are classified into two types based on their gelation processes, either *in situ* gelation or *ex situ* gelation. The *in situ* formed hydrogels have received considerable attention because of their injectable matrices, easy encapsulation of therapeutic agents during formation of the hydrogel network, and their minimal invasiveness into the target site (Fig. 1) [3].

✉ Saji Uthaman
sajiuthaman@gmail.com

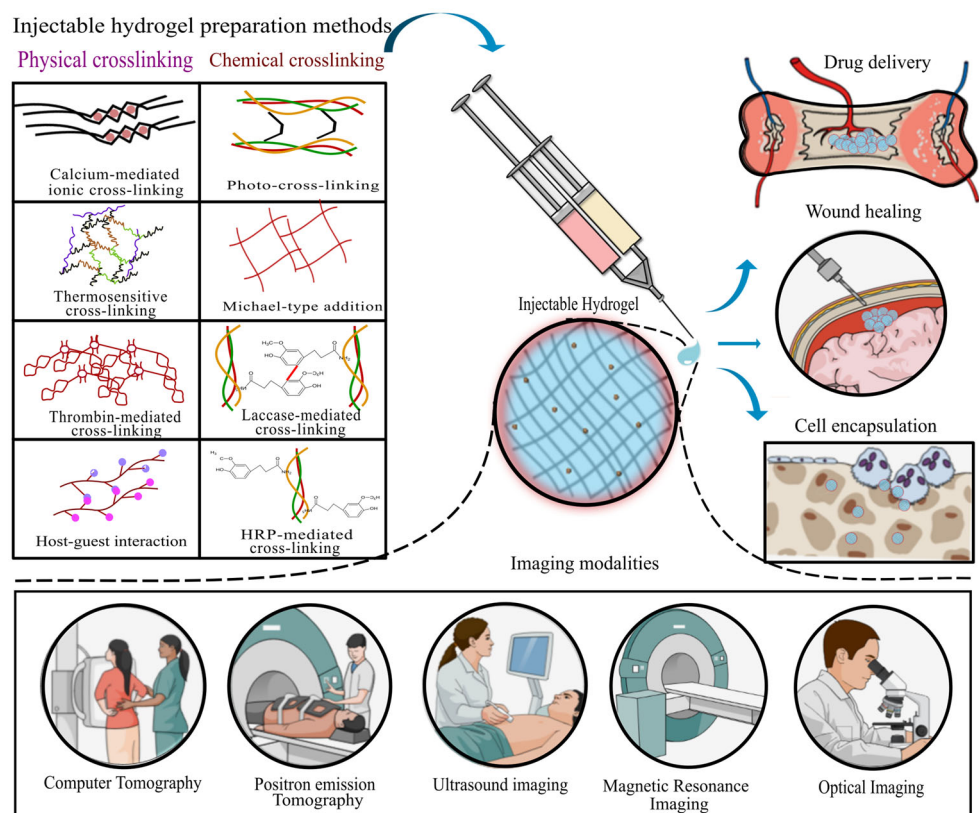
✉ In-Kyu Park
pik96@jnu.ac.kr

¹ Department of Biomedical Sciences, Chonnam National University, Chonnam National University Medical School, 160 Baekseo-ro, Dong-gu, Gwangju 61469, Republic of Korea

² Department of Plastic Surgery, Cleveland Clinic, 9500 Euclid Avenue, Cleveland, OH 44195, USA

³ Department of Polymer Science and Engineering, Chungnam National University, 99 Daehak-Ro, Yuseong-Gu, Daejeon 34134, Republic of Korea

Fig. 1 Schematic representations illustrating the fabrication methods of injectable hydrogels by physical and chemical cross-linking and their biomedical applications and imaging modalities



Various natural, synthetic and hybrid polymers are used in the formation of *in situ* hydrogels. Hydrophilic polymers from natural origins used for the synthesis of hydrogel matrices are anionic polymers (hyaluronic acid, chondroitin sulfate, dextran sulfate, pectin), cationic polymers (chitosan, poly-L-lysine), neutral polymers (dextran, agarose, pullulan), and amphiphilic polymers (collagen/gelatin, carboxymethyl chitin, fibrin) [4]. The properties of injectable hydrogels (Fig. 2), such as responses to physical, chemical, or biochemical changes, physical properties, preparation techniques, source of origin, degradability and cross-linking mechanism, play a very important role in tissue engineering applications.

Based on the mode of cross-linking, injectable hydrogels are classified into physically cross-linked hydrogels and chemically cross-linked hydrogels (Fig. 3). The physically cross-linked hydrogels involve ionic cross-linking, stimuli-sensitive cross-linking (thermoreponsive and pH sensitive) and host–guest interactions [3]. Chemically cross-linked hydrogels are superior to physically cross-linked hydrogels owing to the formation of covalent bonds, which benefit the mechanical properties of the injectable hydrogel. The various chemical cross-linking procedures involves photo cross-linking, Michael-type addition, and enzyme-mediated cross-linking [3]. The merit of physically cross-linked hydrogels is that gelation occurs in mild

conditions without any toxic chemical cross-linking or catalysts. However, the drawback of physically cross-linked hydrogels is their inability to uniformly encapsulate potential drugs and cells because of their weak mechanical properties (viscosity and Young's modulus), which limits their biomedical applications. The most widely used cross-linking to fabricate injectable hydrogels and to include di and tri (e.g., barium, Ba^{2+} , and magnesium, Mg^{2+}) ions is ionic cross-linking [5]. For example, liposomes are designed to cleave at physiological temperature and release calcium ions, effectively cross-linking aqueous sodium alginate via ionic interactions and cross-linking fibrinogen by the *in situ* activity of a calcium-dependent transglutaminase enzyme [6]. The stimuli-sensitive hydrogels are cross-linked in response to pH or temperature. For example, cellulose hydrogels can be prepared by the cross-linking of aqueous solutions of cellulose ethers (e.g., carboxymethyl cellulose (CMC), ethyl cellulose (EC), and sodium carboxymethylcellulose (NaCMC)). Due to the hydrophobic-hydrophilic equilibrium of the thermoresponsive hydrogel preparation, the methyl cellulose (MC) is constant; this equilibrium expands the molecular chain by small changes in temperature [7]. A report of host–guest interactions in a supramolecular hydrogel has recently attracted increased attention [8]. In supramolecular chemistry, the host–guest interaction describes complexes that

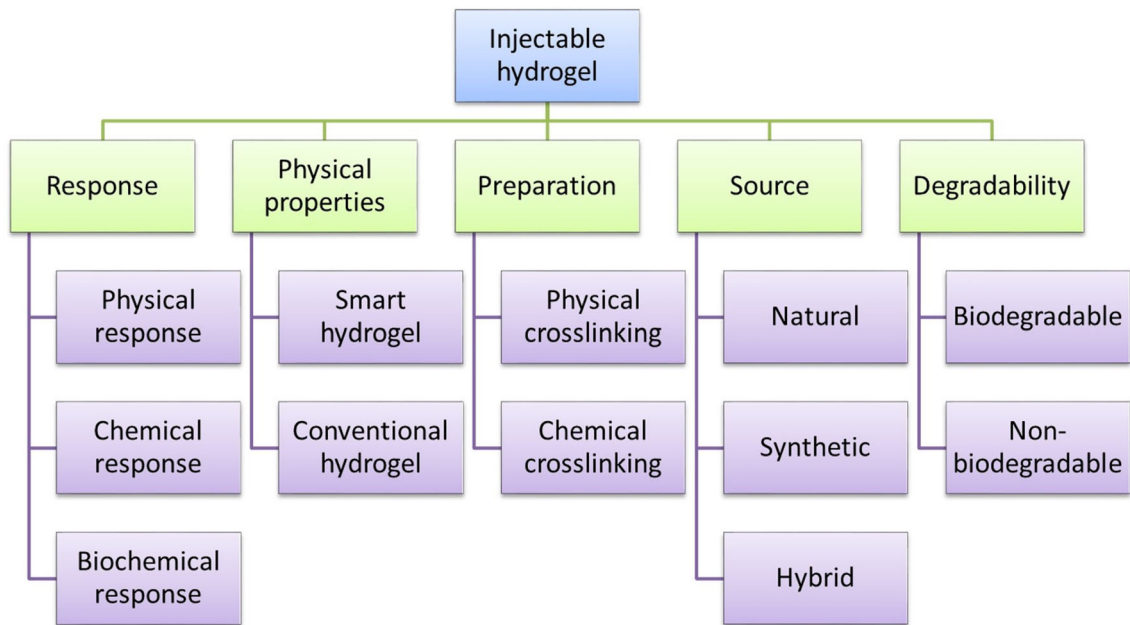


Fig. 2 Classification of injectable hydrogels based on their properties

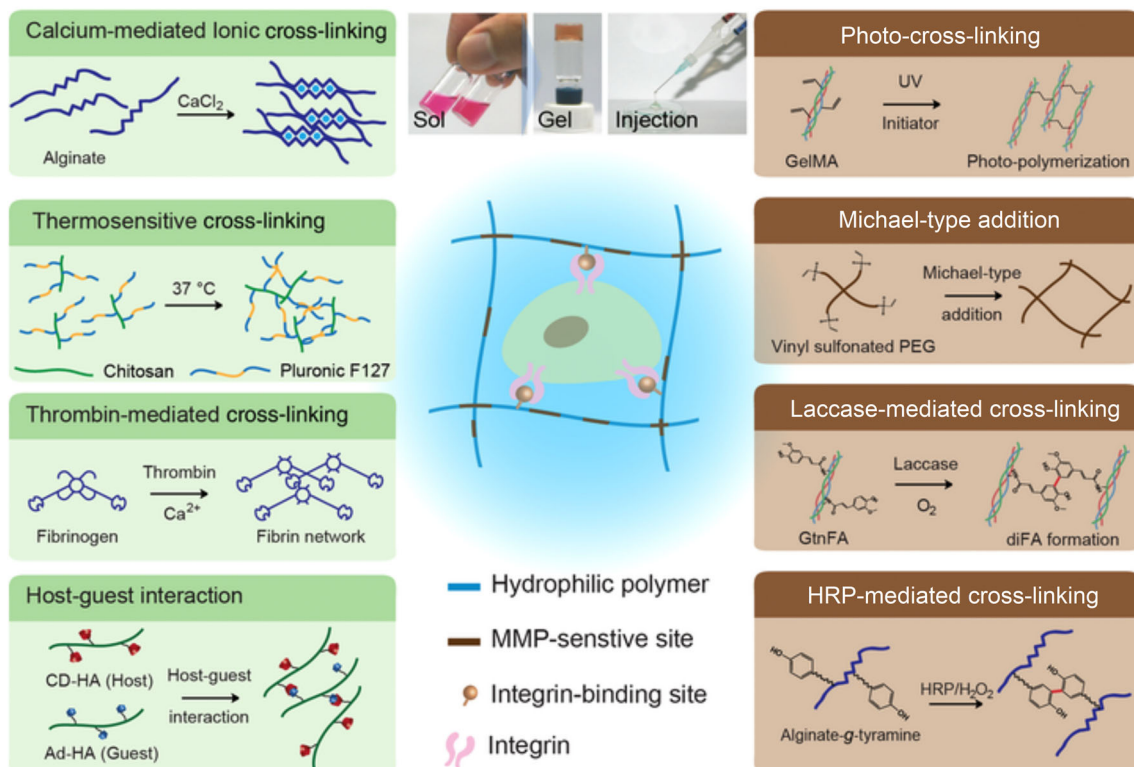


Fig. 3 Schematic representation of the preparation of *in situ* cross-linked hydrogels as injectable matrices via physical and chemical cross-linking reactions. Cross-linking strategies are determined for each hydrogel system. The left side indicates physical cross-linking, and the right side indicates chemical cross-linking reactions.

Horseshadish peroxidase (HRP), β -cyclodextrin-modified hyaluronic acid (CD-HA), ferulic acid (FA), methacrylate gelatin (Gel MA), gelatin grafted with ferulic acid (GtnFA), hyaluronic acid (HA), matrix metalloproteinase (MMP). Duplicated with permission from Ref [3]. Copyright © 2018, John Wiley and Sons

are composed of two or more molecules or ions that are held together in a unique structural relationship by forces other than full covalent bonds. During the past few years, several macrocyclic molecules and their derivatives have been developed such as calixarenes (CAs), cyclodextrins (CDs), and cyclophanes. These macrocyclic molecules are regarded as hosts, possessing cavities that encapsulate the guest [9]. These cavities are loaded with various drugs, imaging agents, or genes, forming an injectable hydrogel that is applicable for drug/gene delivery, bioimaging or photodynamic studies. Compared to physical cross-linking, the covalent bonds formed in chemical cross-linking provide strong mechanical properties to the injectable hydrogel, and the viscosity of the precursor solution is comparatively low, which leads to easy handling and control of the physicochemical properties by optimizing the parameters. Visible and UV irradiation is usually used for the photo cross-linking of injectable hydrogels [3]. The Michael-type addition reaction is the nucleophilic addition of a carbanion or other nucleophile to an α,β -unsaturated carbonyl compound (e.g., vinyl sulfone, α,β -unsaturated esters and maleimides). It is also referred to as a 1,4-type addition and has been broadly utilized in the synthesis of injectable hydrogels [3]. Enzyme-mediated cross-linking is an alternative chemical cross-linking method for the preparation of injectable hydrogels and has the attractive characteristics of being biocompatible and site specific. To create *in situ* hydrogels, various enzymes have been used as a catalyst, such as horseradish peroxidase (HRP), laccase, and transglutaminase.

Hydrogels are widely used for cell growth and tissue engineering due to their high water retention capacity, biocompatibility, and tissue-linked elastic properties [4, 10]. In tissue engineering applications, injectable hydrogels provide good transport of nutrients to cells, *in situ* gelation, good biocompatibility and ease of modification with cell adhesion ligands [11]. The aqueous environment within the hydrogel protects the fragile drugs (peptides, oligonucleotides, DNA and proteins). The prerequisite properties of injectable hydrogels relevant to their usage as matrices for tissue engineering are their degradable or nondegradable nature, mechanical strength, shape and structure/volume ratio, water content and charge, chemical modifications (presence of attached cell adhesion ligands), added bioactive components (cells, drugs) and serializability [4].

Compared with conventional scaffolds, injectable hydrogels possesses greater advantages, such as ease of handling, requiring minimal invasiveness, deep penetration efficiency, excellent defect margin adoption and complete defect filling, while the conventional scaffolds are comparatively difficult to handle, with the need for invasive surgeries, lower tissue penetration depths, improper defect

margin adoption and incomplete defect filling [11]. In tissue engineering, injectable hydrogels also play a primary role in bioimaging applications, because these bioactive hydrogels can be imaged by various imaging modalities (Fig. 1), such as optical imaging, positron emission tomography (PET), ultrasound, magnetic resonance imaging (MRI) and computer tomography (CT). In this review, we discuss the different types of biopolymeric injectable hydrogels, modes of preparation, biopolymers used for tissue engineering applications, and *in situ* imaging techniques using injectable hydrogels.

2 Injectable hydrogels as bioactive materials

2.1 Bioactive injectable hydrogels of natural origin

Bioactive injectable hydrogels of natural origin have been widely studied because of their excellent biodegradability and biocompatibility. Natural biomaterials frequently used in the fabrication of injectable hydrogels are cellulose [12], chitosan [13], collagen/gelatin [14, 15], alginate [16], and hyaluronic acid [17].

2.2 Cellulose-derived injectable hydrogels

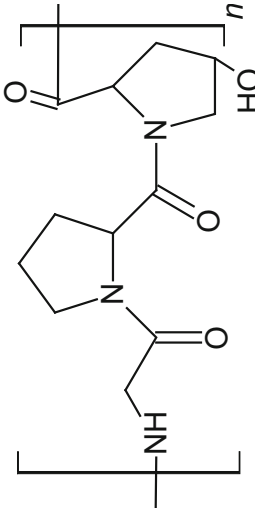
Cellulose is a biopolymer that is abundantly found in nature. It is a straight chain polysaccharide containing D-anhydroglucopyranose units joined together by β -1,4-glucoside bonds (Table 1). The intramolecular and intermolecular hydrogen bonds present in cellulose make it insoluble in water [18]. At low temperatures, cellulose forms hydrogels and has a high-water solubility due to the entrapment of water molecules through the hydrogen bonds. As the temperature increases, the hydrogen bonds are cleaved, thus exposing the methoxy groups, and breaks exposing the methyl group lead to hydrophobic interactions that subsequently result in the formation of a three-dimensional hydrogel network [18].

The gelation temperature of cellulose-derived hydrogels is lower than body temperature, making them a suitable candidate for *in situ* hydrogel applications. These hydrogels can be loaded with bioactive drugs or nanoparticles in aqueous phase and be remodeled into the specified shape upon *in vivo* administration [17]. To enhance the physical and chemical properties of the injectable hydrogel, Deng et al. [12] prepared cellulose-based hydrogels that were *in situ* cross-linked with hyaluronic acid and carboxymethyl cellulose via a disulfide bond formed by the oxidation of dissolved oxygen. The resulting injectable hydrogel showed a tunable gelation time, appropriate physical properties, a high swelling quantitative relation, adaptability, and sustained drug release

Table 1 Biopolymers preparation, gelation method and their tissue engineering applications

Natural polymer	Chemical structure	Gelation method	Types of encapsulation cells	Tissue engineering applications	References
Cellulose		Thermal cross-linking	Cartilage cells	Wound healing, drug delivery	[12, 18, 38]
Chitosan		Free radical polymerization/chemical/Michael-type addition/thermal cross-linking and pH-induced cross-linking	Human MSCs, chondrocytes	Encapsulate hepatocytes, orthopedic scaffolds	[17, 21–23, 41]
Collagen		Thermal cross-linking, chemical cross-linking	Human MSCs, chondrocytes, cardiomyocytes, osteoblast	Wound healing, promote blood coagulation, the scaffolds for cell	[24, 27, 35]
Hyaluronic acid		Free radical polymerization, Michael-type addition	Human MSCs, chondrocytes, fibroblast	Cartilage regeneration, wound healing	[15, 17, 23, 30]
Alginate		Ionic interaction, free radical polymerization	Human MSCs, hepatocytes	Wound healing, cartilage regeneration	[5, 16, 35, 38–40]

Table 1 continued

Natural polymer	Chemical structure	Gelation method	Types of encapsulation cells	Tissue engineering applications	References
Gelatin		Heating/cooling polymer solution solid state redaction	Human MSCs	Support cells for orthopedic applications	[21, 29, 42]

ability. Chitosan is a natural derivative of chitin, which is a linear polysaccharide chain composed of *N*-acetyl-D-glucosamine and glucosamine [17]. Zhou et al. [19] prepared *N*-methylmorpholine-*N*-oxide monohydrate (NMMO), which is an effective green solvent for cellulose in industries for the preparation of fibers. This compound demonstrated a high thermal stability, low toxicity and the possibility of reusability. To enhance the physical and chemical properties of the injectable hydrogel, Deng et al. [12] have prepared cellulose-based hydrogel that was *in situ* crosslinked with hyaluronic acid and carboxymethyl cellulose by the oxidation of dissolved oxygen via disulfide bonds. The resulting injectable hydrogel showed a tunable gelation time, applicable physical properties, high swelling quantitative relation, adaptability, and sustained drug release property.

2.3 Chitosan-based injectable hydrogels

Chitosan is a natural derivative of chitin, which is a linear polysaccharide chain composed of *n*-acetylglucosamine and glucosamine [17]. Chitin undergoes deacetylation to produce *D*-glucosamine units randomly within the polymer chains of *N*-acetyl-*D*-glucosamine (Table 1). Chitosan is one of the most widely investigated polymers for tissue engineering applications because of its physicochemical characteristics, such as biodegradability, hydrophilicity, mechanical strength, and biocompatibility [20]. Injectable chitosan-based hydrogels can encapsulate cells through the electrostatic interactions between the anionic cell membranes and amino groups in chitosan [21]. Chitosan forms gels by various gelation methods such as free radical polymerization, Michael-type addition, thermal cross-linking and pH-induced cross-linking (Table 1). In improving the bioactive properties of chitosan, researchers have combined chitosan with various natural polymers such as cellulose and gelatin to make composites [20, 22]. To enhance the tissue adhesiveness, antibacterial and hemostatic properties of chitosan hydrogels, Lu et al. [13] fabricated an *in situ* gelation complex composed of glycol chitosan that was photochemically cross-linked; the complex shows good tissue adhesiveness and controlled drug release capabilities. Zhang et al. [23] developed chitosan/hyaluronic acid/sodium glycerophosphate-based injectable hydrogels, which possess temperature and pH sensitivity for drug release and can attach to cancer cells.

2.4 Collagen-based injectable hydrogels

Collagen is a primary protein found in the extracellular matrix of different connective tissues and is one of the most common proteins in mammals, making up to 25 to 35% of total body proteins. There are at least 29 types of collagens, and all display a helical structure with defined

patterns of amino acids [24]. Collagen is the preferred material for neural tissue engineering approaches due to its similarity to the extracellular matrix and its biocompatibility and antigenicity. Collagen-based biomaterials originate from two fundamental techniques. The first is a decellularized collagen matrix that maintains the primary tissue morphology and extracellular matrix morphology, while the second depends on the derivation from biological tissues (porcine skin and bovine) for the formation of functional scaffolds [24]. Collagen hydrogels also have superior biodegradability, bioactivity, and biocompatibility, which have made them an interesting material for biomedical applications. Yuan et al. [14] have prepared a favorable injectable hydrogel by combining type I and type II collagen in which the compressive modules can be regulated by exchanging the type I and type II collagen composition. Latifi et al. [25] prepared an injectable hydrogel with a semi-interpenetrating polymeric network of heterotopic fibril collagen that has specificity towards tissues such as type III collagen, with a tissue-specific collagen-III to collagen-I ratio in a glycol-chitosan matrix. Collagen-I has an influence on fibrogenesis in terms of mechanics and diameter, and it is mechanically stable under continuous dynamic stimulation. These hydrogels provide an extended half-life that is greater than that of hyaluronic acid-based hydrogels. These hydrogels also support cell viability, adhesion, migration and metabolic activity. Collagen-based injectable hydrogels are highly applicable in wound healing, promote blood coagulation and can be used as scaffolds for cells (Table 1) [26, 27].

2.5 Gelatin-based injectable hydrogels

Gelatin is a natural protein that is extracted by the thermal degradation of collagen and possesses thermoresponsive properties. It solidifies at temperatures less than 25 °C, and when the temperature increases above 30 °C, the hydrogel changes to a liquid [21]. Gelatin-based injectable hydrogels possess high biocompatibility and biodegradability in the physical environment. Geng et al. [28] fabricated injectable hydrogels, using oxidized dextrin, 4-armed PEG-acrylate and amino gelatin for the encapsulation of cells. The spreading and proliferation of cells within the injectable hydrogel was high, and the hydrogel showed favorable mechanical properties, biocompatibility, and biodegradability. To reduce the degradation rate of the injectable hydrogel, Hozumi et al. [15] cross-linked gelatin and hyaluronic acid in a Schiff base formulation to delay degradation of the composites, which is suitable for the induction of angiogenesis. Gelatin is an FDA-approved natural polymer in the dural repair technique that closes significant dural gaps, in which a gelatin or collagen sponge is applied. However, it is not advised to use these

hydrogels to conform to bony structures where nerves are present, since neural compression may result due to hydrogel swelling. The hydrogel may swell up to 50% of its size in any dimension. Gelatin-based hydrogels are commonly applied to provide cell support in orthopedic applications [29].

2.6 Hyaluronic acid-based injectable hydrogels

Hyaluronic acid is a natural polymer and nonimmunogenic polysaccharide that exists in various parts of the body as a component of the extracellular matrix of the human skin. It plays a vital role in most tissues and cellular functions and has been clinically used for many years, mainly in wound healing applications. The hyaluronic acid polymer can be chemically modified into different physical forms, such as soft or stiff hydrogels, viscoelastic solutions, nonwoven meshes, electrospun fibers, nanoparticle fluids and flexible sheets for implementation in preclinical and clinical settings. Many different forms of hyaluronic acid have been derived via the cross-linking of pendant reactive groups, by addition/condensation chemical reactions, or by free radical polymerization [30]. Due to the poor mechanical properties of hyaluronic acid, it is often modified or combined with other biomaterials for use in practical applications. hyaluronic acid has been self-cross-linked with hydrazide-functionalized poly (γ -glutamic acid) for the delivery of protein and formed *in situ* hydrogels within 9 s, with a high swelling ratio and rheological properties, illustrating an extensive processing range with high mechanical strength [31]. hyaluronic acid has also been used to enhance angiogenesis via an injectable chitosan-hyaluronic acid-based hydrogel that was incorporated with proangiogenic molecules (deferioxamine-loaded polylactide-co-glycolic acid nanoparticles) using the double emulsion solvent diffusion technique [32]. The hyaluronic acid-based injectable hydrogel showed excellent cytocompatibility and good cell proliferation for rASCs (rat adipose-derived stromal cells) and HUVECs (human umbilical vein endothelial cells). *In situ* cross-linked hyaluronic acid hydrogels created via a biorthogonal reaction show a potential clinical application for *in vivo* cartilage regeneration. Han et al. have synthesized an *in situ* cross-linked and injectable hyaluronic acid-PEG-dibenzocyclooctyl (DBCO) hydrogel for tissue engineering applications using a simple biorthogonal click reaction. The hydrogels showed good biocompatibility during *in situ* physical gelation and supported cell survival and cell regeneration of cartilaginous tissue [33].

2.7 Alginate-based injectable hydrogels

Alginate, extracted from brown algae (phaeophyte), is polysaccharide consisting of guluronic and mannuronic acid. It is a naturally occurring compound that exhibits cross-linking ability with di- or trivalent cations. Calcium chloride is a common ionic interaction crosslinker that has been used as a cross-linking agent. The calcium (Ca^{2+}) ions bind to the guluronate monomers of the alginate polymer, which results in junction formation with a guluronate block of the adjacent polymer chain, thereby forming a gel. The major disadvantage of the ion cross-linked gelation system is that the ions interchange with ionic molecules in aqueous environments, leading to weakening of the properties of the injectable hydrogel [34]. Alginate hydrogels have been used for the sustained release of bone morphogenetic protein-2 (BMP-2) [35] and also in wound healing applications [16, 35]. Liao et al. [16] fabricated a hybrid alginate-based injectable hydrogel by ionic cross-linking using calcium gluconate crystals deposited in poly (ϵ -caprolactone)-*b*-poly (ethylene glycol)-*b*-poly (caprolactone). The hydrogel possessed good flexibility, even at a concentration of 500 $\mu\text{g}/\text{ml}$, owing to higher cell viability.

2.8 Clinical applications of injectable hydrogels

The clinical applications of injectable hydrogels are limited in number, and only a few of them are FDA-approved commercial products. Most of these are used in healing ocular surgery incisions. The clinical use of regenerative hydrogels and drug-delivery injectable hydrogels is under investigation, however, progress in this research area is relatively slow [36]. Cellulose hydrogel has been clinically used in bone graft material in combination with glycerin,

water and plant-derived sodium carboxymethylcellulose (NACMC) [37]. Alginate is a cationic biopolymer that forms physically cross-linked hydrogels in the presence of divalent cations. It has been used in several clinical applications, including wound dressing materials [38], and was the first material to enter clinical trials for the treatment of myocardial infarction [39]. Alginate-based injectable hydrogels have been utilized in the regeneration of various tissues, including bone, cartilage, adipose and cardiac tissues [40]. Chitosan injectable hydrogel that has been enzymatically cross-linked with glycol is used as a delivery vehicle for the support of bone and cartilage regeneration. This injectable hydrogel was novel in its use for minimally invasive applications, and it provides a mild environment for the encapsulation of cells, drugs and other biological factors for release at local, injured sites to promote tissue healing [41]. Gelatin hydrogel is used for sealing peripheral arterial or venous reconstructions. A total of one hundred forty eight patients were treated with this hydrogel, and the success rate was equivalent to that of the control (absorbable gelatin sponge/thrombin hemostat) group. There was no report of unanticipated adverse effects related to the hydrogel sealant in this investigation [42]. Hyaluronic acid hydrogel is clinically used in wound healing for leg ulcers, pressure ulcers, diabetic ulcers, surgical wounds, mechanically or surgically debrided wounds and second-degree burns.

3 *In situ* hydrogels for bioimaging applications

Bioimaging plays a crucial role in understanding the morphology, structure, metabolism, and functions of cells. Characteristics to be considered for an ideal imaging agent

Table 2 Imaging modalities of injectable hydrogel and their tissue engineering applications

Imaging modalities	Source	Typical penetration depth	Contrast agents and molecular probes	Spectral resolution	Gelation method	Tissue engineering applications	References
Computer tomography	x-ray	>10 cm	Iodine, barium	12–50 μm	Thermal	Prevention of fragile fracture, bone regeneration	[49, 51–53]
PET/Micro-PET	γ -rays	>10 cm	Fluorodeoxyglucose (FDG) ^{18}F , ^{11}C , ^{15}O	1–2 mm	Cross-linking	Tissue regeneration	[43, 47, 50, 56]
Ultrasound	Acoustic reflection	0.1–10 cm	Microbubbles, nanoparticles	50 μm	Self-assembling, thermal	Bone regeneration	[44, 46, 57, 58]
Magnetic resonance imaging	Radio wave	>10 cm	Gadolinium, dysprosium, iron oxide particles	4–100 μm	Charge-based cross-linking	Regenerative medicine, drug delivery	[45, 48, 60–68]
Optical imaging	light	Several mm		>0.3 μm	Charge-based cross-linking	Regenerative medicine, drug delivery	[66, 69, 73]

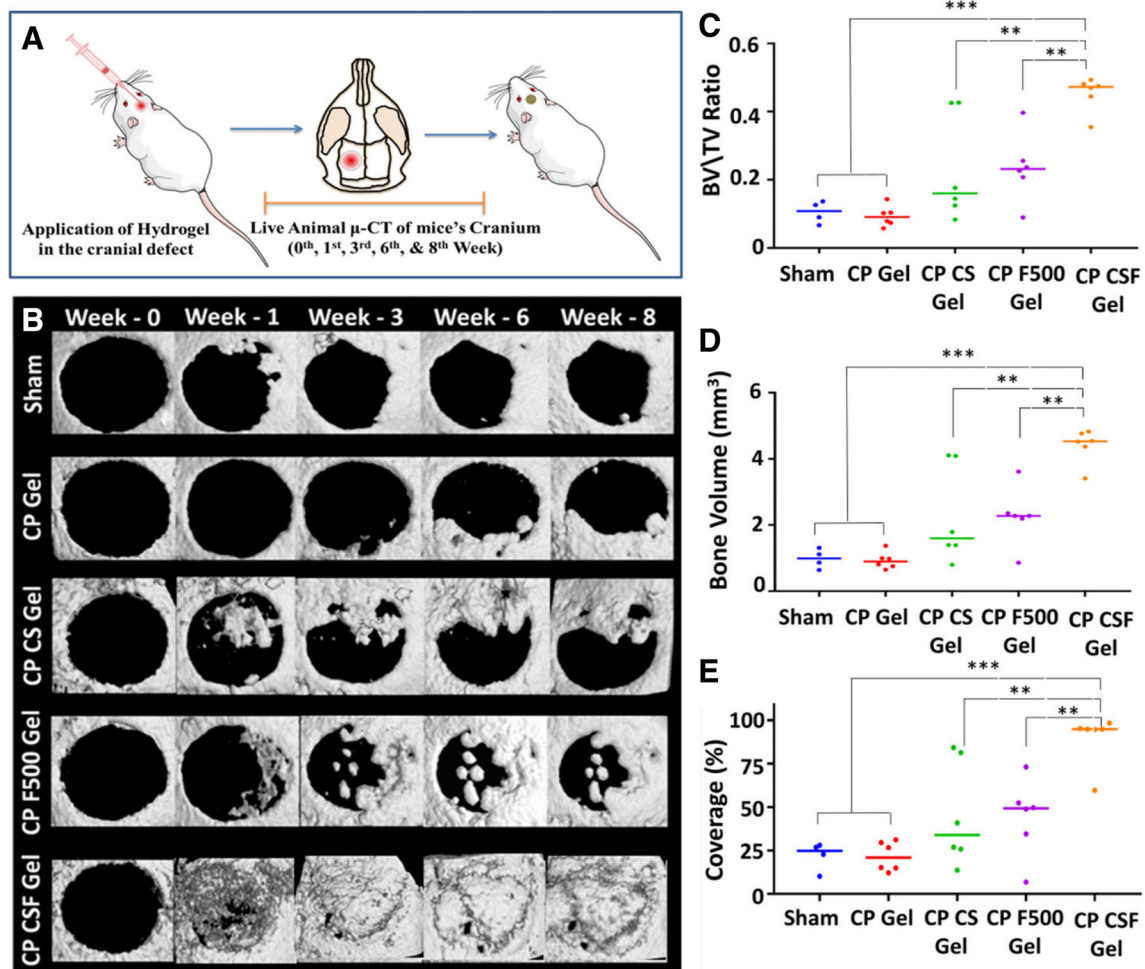


Fig. 4 Schematic representation showing the *in vivo* animal study and application of chitin-PLGA-injectable hydrogel in bone regeneration. **A** Schematic representation of the *in vivo* animal study. **B** Living animal μ -CT imaging of mice at the zero, first, third, sixth and eighth week for the sham control, CP gel, CP CS gel, CP F500

gel, and CP CSF500 gel. **C** Bone volume (BV)/total volume (TV) ratio measured by the bone module at the end of the eighth week. **D** BV and **E** coverage (%) in the defect area at 8 weeks. Reproduced with permission from Ref. [53]. Copyright © 2017, American Chemical Society

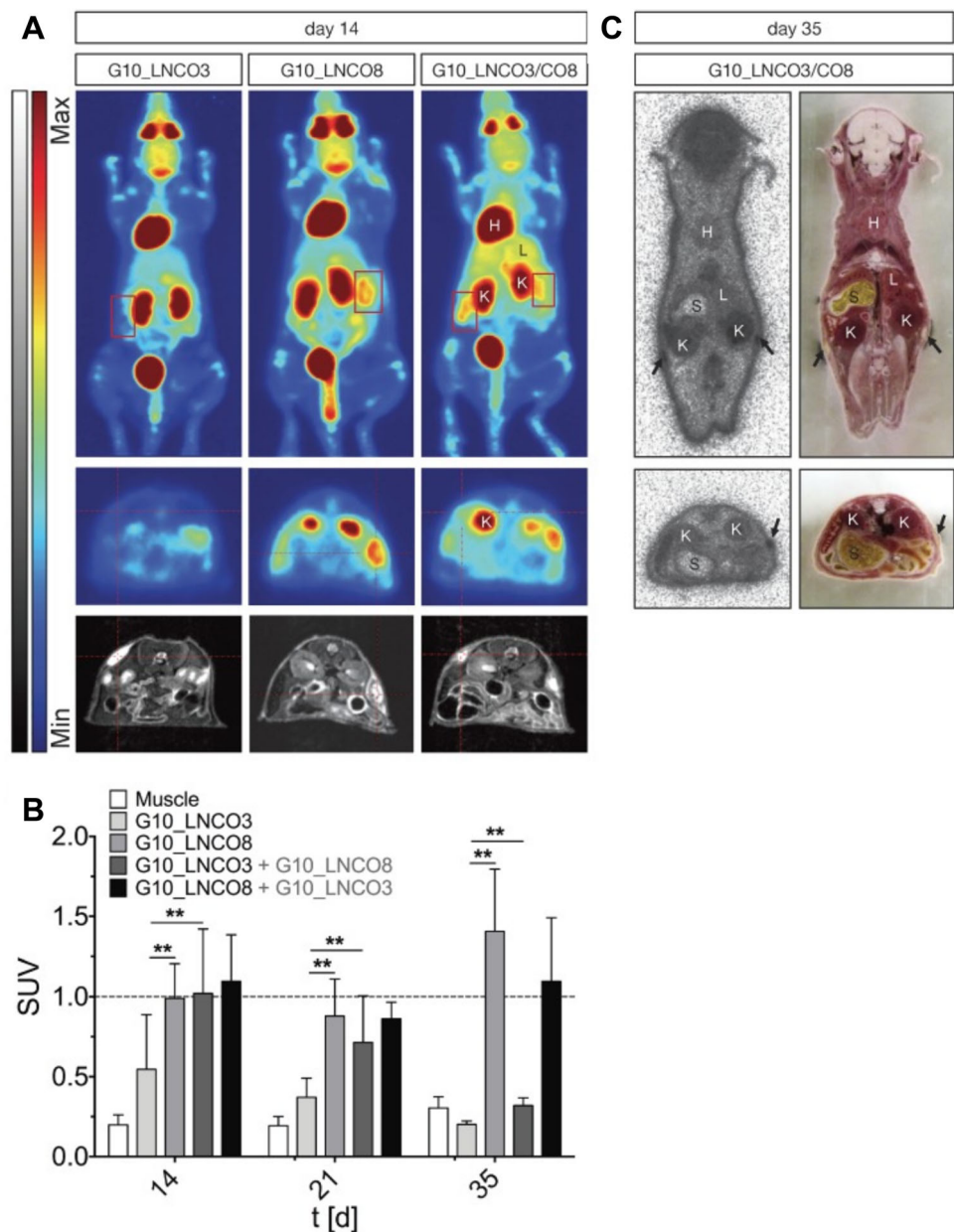
include sensitivity, specificity, efficiency, optimal clearance and response to disease biomarkers to assist in the diagnosis, assessment and treatment of diseases. Image-guided drug delivery has been widely investigated to incorporate chemotherapeutic drugs with different imaging modalities such as single-photon emission computed tomography (PET) [43], ultrasound (US) [44], magnetic resonance imaging (MRI) [45] fluorescence imaging [46] and positron emission tomography (PET) [47]. Among these, MRI is one of the most commonly used diagnostic methods due to its superior spatial resolution and soft tissue contrast [48].

3.1 Computer tomography (CT)

In CT, the intrinsic differences of X-ray absorbance among, fat, air, bone and water provide contrast. To obtain

volumetric information, CT uses low-energy X-ray sources and a rotating detector, which rotates around the subject (Table 2). The detectors are charged, coupled devices that react to photo transducer incoming X-rays [49]. In clinics, the use of higher X-ray energies should be minimized because when patients are exposed to these higher energies, the additional ions that are generated may result in adverse health effects. The contrast of CT is low in tumors and surrounding tissues. However, with the help of iodinated contrast agents, organs and tumors can be analyzed [50]. Because of the similar atomic composition of living tissues (other than bone) and hydrogels, their X-ray absorbances are more closely aligned. To distinguish living tissue from a hydrogel, high atomic number elements must be incorporated into the hydrogel to enhance the contrast between them. The commonly used X-ray agents are barium and iodine, as they have good X-ray radiopacity and have been

Fig. 5 Fluorodeoxyglucose (FDG) PET imaging and quantification. **A** Maximum intensity of coronal projection (0–60 min, upper panel) and transversal projection (30–60 min, mid panel) for dynamic PET experiential with [^{18}F] FDG coregistered to MRI projection (lower panel) 14 days after implantation of either G10_LNCO3 (left panel), G10_LNCO8 (mid panel), or both (right panel). **B** Mean Standardized uptake values (SUV) of [^{18}F] FDG (30–60 min p.i.) on day 14, 21 and 35 after hydrogel implantation. **C** Autoradiography of double-implanted mice 35 days after implantation (upper panel). The transversal section is shown in the lower panel. The left side shows autoradiography. The whole-animal cryo-section is shown on the right side. This image was taken from the copyright © 2018 Ivy Spring International Publications [56]



proven to be efficient in increasing the contrast [51]. Tan et al. [52] developed an injectable hydrogel composed of thermosensitive simvastatin/Poloxamer 407 for the CT-guided percutaneous intraosseous injection into extended vertebrae in ovariectomized minipigs for osteoporosis treatment to prevent fragile fracture. Sivashanmugam et al. [53] fabricated an injectable hydrogel composed of a poly (lactide-co-glycolide) chitin-PLGA hydrogel (CP Gel) complex formed by regeneration chemistry and later combined with FGF-18 and CaSO_4 (CS) for bone regeneration. These results demonstrated the successful longitudinal μ -CT imaging of live animals, as shown in Fig. 4.

3.2 Positron emission tomography (PET)

PET uses radioactive tracking molecules that are incorporated into metabolically active molecules, such as labeled spiperone in pituitary adenomas that target dopamine receptors. PET is used in biological imaging studies concerning bone metabolism [43] and metastasis, which is a common phenomenon for most cancers, including lung, prostate, and breast [54]. The merits of PET include that it is a minimally invasive technology and is highly sensitive, and it is ideally suited for clinical and preclinical imaging. 3D images can be constructed using radioactive tracers [55]. However, its spatial resolution is relatively low (Table 2), and it is restricted by pixel sampling quantity,

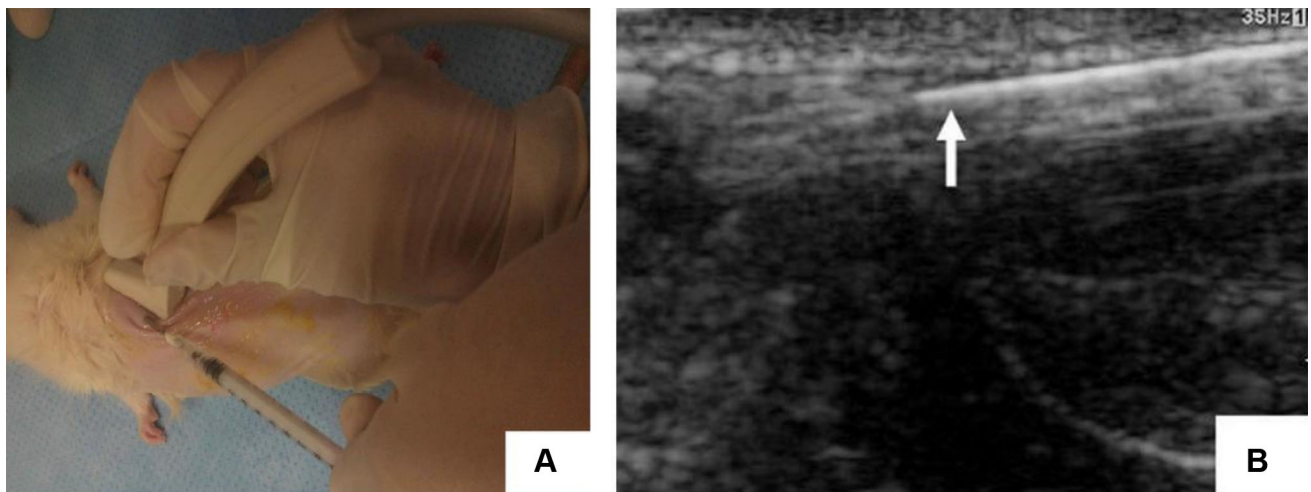


Fig. 6 Ultrasound image of the injection process of the *in situ* formation of chitosan and chitosan-hydroxyapatite hydrogels. **A** Subcutaneous injection of the hydrogel under ultrasound transducer.

B Monitoring of the injected ultrasound (arrow indicated the syringe needle). This image was taken from the Journal of Nanomaterials [59] copyright © 2012, Yan Chen et al.

blurring in the phosphor screen of the detector and the source size. Tondera et al. [56] prepared a gelatin-based hydrogel, where the gelatin was cross-linked with lysine diisocyanate ethyl ester (LDI), and the molar proportion of LDI and gelatin in the primary material blend dictated the flexible properties of the subsequent hydrogel. In order to investigate the clinical potential of these biopolymers, hydrogels with different ratios of gelatin and diisocyanate (3-folds (G10_LNCO3) and 8-folds (G10_LNCO8) molar excess of isocyanate groups) were subcutaneously implanted in mice. The biomaterial-tissue-interaction and degradation were explored *in vivo* by optical imaging, MRI and PET. The PET imaging was carried out via small animal PET after the intravenous injection of [^{18}F] fluorodeoxyglucose, as shown in Fig. 5.

3.3 Ultrasound imaging

Ultrasound (US) is an imaging technique commonly used to produce 3D biological images of newly formed tissue and engineered tissue up to depths of ten centimeters [57, 58]. US is considered to be the safest imaging modality due to its low acoustic wave energy and high imaging speed and penetration depth. The interaction of biomaterials with the surrounding tissue, including their modulus, mass densities and cavities in a collagen hydrogel, have been widely studied by US imaging, along with the physical and morphological properties [46]. Doppler US imaging has been used to track the flow of dynamic fabrication in vascular grafts and the visualization of the injectable hydrogel *in vivo* [59]; however, US imaging has two drawbacks: it lacks sensitivity to the functional and molecular status of engineered tissue biomaterials because of its mechanically distinct mechanism, and due to the long

acoustic wavelength used for the formation of the image, the spectral resolution can only reach single cell levels. In particular, US has been widely used in tissue engineering for visualizing injected biomaterials. Chen et al. [59] demonstrated that US could be used for nondestructive, noninvasive monitoring and for assessing the *in vivo* characteristics of injectable, *in situ* formed hydrogel-based bone scaffolds. They also demonstrated the use of nanohydroxyapatite, collagen and chitosan *in situ*-formed hydrogels that show good rigidity, low degradation rates and improved blood supply *in vivo*, as evaluated by US as shown in Fig. 6.

3.4 Magnetic Resonance Imaging (MRI)

MRI is an imaging modality used in the medical field that uses radiology to construct an image of the physiology and anatomy of the body for healthy and disease conditions. Interestingly, MRI is relatively safe, as it does not use any ionizing radiation [60, 61]. It applies high magnetic fields, radio frequencies and electric fields to generate images of bodily organs. Proton longitudinal relaxation (r_1) and transverse relaxation (r_2) are the constraints used to estimate the contrast agent for MRI; the contrast agent can be determined by the change in the proton longitudinal relaxation time (T1) and the transverse relaxation time (T2) of water.

MRI can be used to characterize the fluid content or proton density of an object [44]. This technique is used in tissue engineering for monitoring the growth of developed material, along with cartilage [62], adipose [63], and vasculature [64], using exogenous or endogenous contrasting agents [65]. Magnetic resonance imaging is a nonionizing and noninvasive analysis, and hence it is utilized in *in vivo*

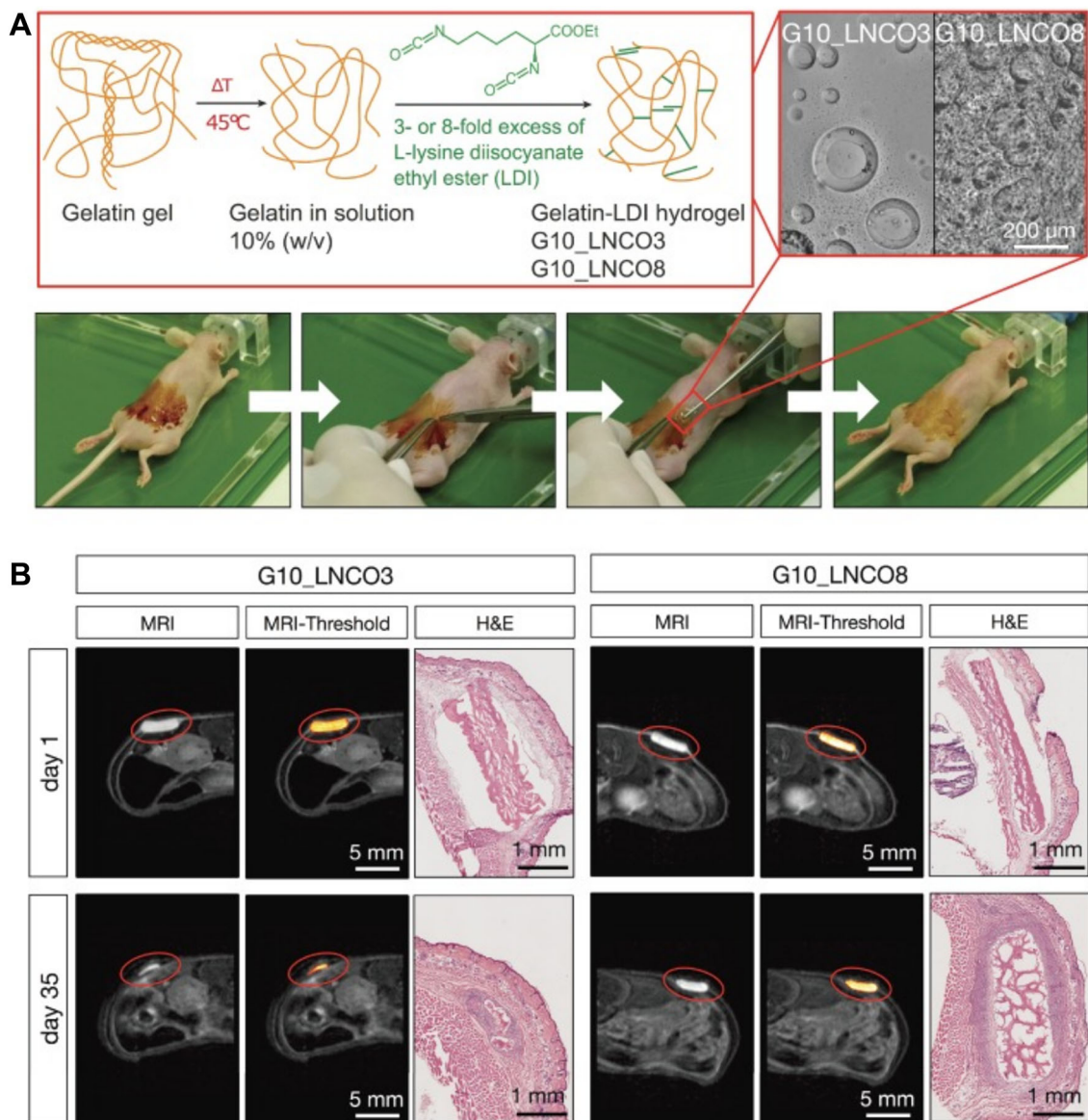


Fig. 7 Visualization of implanted hydrogel (**A**). Scheme of the gelatin-based injectable hydrogel at different ratios of gelatin and diisocyanate [3-fold (G10_LNCO3) and 8-fold (G10_LNCO8) molar excess of isocyanate group]. The confocal image showed the different surface structures of the different hydrogels. Implantation is shown in the lower image. First, the mouse skin was disinfected, then an incision formed a skin pocket and the preswollen hydrogel was implanted. Finally, the incision was closed using spray-plaster.

B Representation of the axial MRI images on day 1 and day 35 after implantation. After drawing a volume of interest around the material (circle) and applying a threshold (middle panel), the volume of the hydrogel could be calculated. Hematoxylin & eosin staining confirmed the difference in degradation of G10_LNCO3 and G10_LNCO8 at 35 days after implantation. This image was taken from Ivy Spring International Publication [56]

studies of biomaterial-tissue interactions, with an increase in the magnetic field ($> 7T$) to improve spatial resolution [66]. MRI has also been applied to track stem cell degradation and the differentiation of engineered scaffolds and hydrogels with specific macromolecules that were bound by superparamagnetic iron-oxide nanoparticles [60, 67, 68]. Bakker et al. fabricated an *in situ* injectable gelation hydrogel that can be visualized by MRI. A supramolecular system with a ureidopyrimidinone-based

injectable hydrogel was entrapped with a modified gadolinium (III)-DOTA complex for enhanced MRI contrast [45]. As previously discussed for PET imaging, Tondera et al. [56] prepared a gelatin-based hydrogel. The biomaterial-tissue-interactions and degradation were examined *in vivo* by optical imaging, MRI contrast, and PET imaging. To evaluate the volume of an implanted hydrogel with MRI, a specific designation T2-weighted estimation sequence was performed, as shown in Fig. 7.

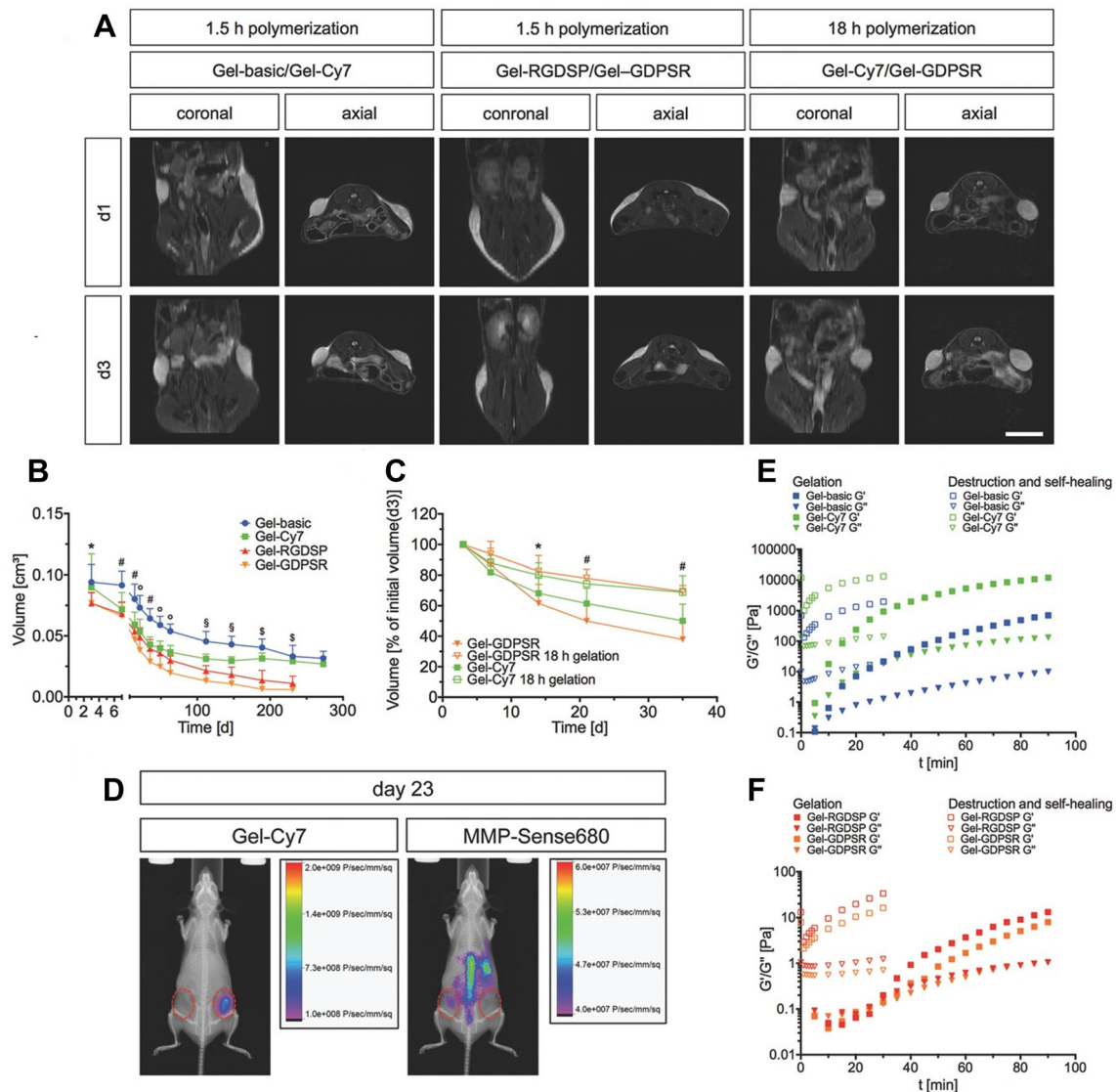


Fig. 8 Hydrogel volumes and degradation rates were determined using small animal MRI. **A** Visualization of the hydrogels utilizing small animal MRI with a T2 weight TRARE-estimating sequence. Compared are the hydrogel volume and body liquid accumulation at 1.5 h after hydrogel injection. Scale bar: 1 cm. **B** Graphical visualization of hydrogel volume determined by MRI over time of mice that were injected 1.5 h after hydrogel preparation. **C** Same as (**B**) but comparing hydrogels injected into mice after 1.5 and 18 h.

3.5 Optical imaging

Optical imaging has become an essential tool for many biological applications because of its flexibility in imaging contrast, high spatial resolution, and ease of operation. Confocal microscopes have been extensively used to topically image cells and tissues *in vivo* and *in vitro* by using fluorescence markers [66]. Depending on the autofluorescence of nicotinamide adenine dinucleotide hydrogen (NADH) in intracellular regions, the cell survival

D Matrix metalloproteinase (MMP)-specific fluorescence agent MMP-Sense 680 ($\lambda_{ex} = 650$ nm, $\lambda_{em} = 700$ nm) showed no specific fluorescence 23 days after Gel-basic and Encapsulated IR fluorescent KA7–Cy7 in Gel-basic (Gel-Cy7) injection. Gelation and self-healing properties of **E** Gel-basic, Gel-Cy7, Gel-RGDSP Peptide and its scrambled sequence (GDPSR) are shown. Duplicated with permission from Ref [73] copyright © 2018, John Wiley and Sons

in 3D scaffolds could be determined [69]. Photoacoustic tomography has been shown to be advantageous in evaluating *in vivo*-injectable hydrogels for the study of tissue angiogenesis and hemoglobin oxygenation saturation [70, 71]. Optical coherence tomography is based on light scattering contrast and is insensitive to the chemical composition of the sample; it is considered to be a powerful tool for the evaluation of 3D structural changes in engineered scaffolds caused by biomaterial degradation and tissue matrix deposition [72]. Generally, due to the strong

optical attenuation of biological and tissue biomaterials, optical imaging is limited by shallow penetration depths, even though it is the dominant characterization technique used in biomaterial-tissue engineering. Tondera et al. [73] prepared an injectable hydrogel system that is cross-linked by peptide-oligosaccharide noncovalent interactions. This dynamic network showed fast self-healing and the ability to be injected. The prepared hydrogel and the release of its encapsulated compounds were monitored in immunocompetent mice for up to 9 months by MRI and optical imaging. These stable hydrogels did not cause an adverse inflammatory response, as measured by MRI, cytokine levels and immunohistochemistry methods, as shown in Fig. 8. These hydrogels possessed high biocompatibility and stability. They could be applicable to regenerative medicine and drug delivery systems.

4 Conclusions and future perspectives

Over the past few years, studies on the rational design of bioactive and injectable biopolymeric-derived hydrogels from cellulose, chitosan, collagen, hyaluronic acid, alginate and gelatin have produced significant progress in the development of bioactive and biocompatible injectable hydrogels. Injectable hydrogels that can be imaged *in vivo* have also been significantly improved. However, it remains necessary to develop next-generation injectable hydrogels that are compatible with the surrounding tissue and do not cause side effects after injection into the body. The further development of hydrogels that can be imaged *in vivo* is critical.

Acknowledgements This work was financially supported by the Basic Science Research Program (No. 2016R1A2B4011184 and 2017R1C1B1003830) and the Bio & Medical Technology Development Program (NRF-2017M3A9E2056374) through the National Research Foundation of Korea (NRF) funded by the Korean government, MSIP. IKP also acknowledges the financial support from a grant (HCRI 17901-22) Chonnam National University Hwasun Hospital Institute for Biomedical Science.

Compliance with ethical standards

Conflicts of interest The authors have no financial conflicts of interest.

Ethical statement There are no animal experiments carried out for this article.

References

1. Campoccia D, Doherty P, Radice M, Brun P, Abatangelo G, Williams DF. Semisynthetic resorbable materials from hyaluronan esterification. *Biomaterials*. 1998;19:2101–27.
2. Prestwich GD, Marecak DM, Marecek JF, Vercruysse KP, Ziebell MR. Controlled chemical modification of hyaluronic acid: synthesis, applications, and biodegradation of hydrazide derivatives. *J Control Release*. 1998;53:93–103.
3. Park KM, Park KD. Injectable hydrogels: properties and applications. In: Chatgililoglu C, Studer A, editors. *Encyclopedia of radicals in chemistry, biology, and materials*. 2017. <https://doi.org/10.1002/0471440264.pst663>.
4. Hoffman AS. Hydrogels for biomedical applications. *Adv Drug Deliv Rev*. 2012;64:18–23.
5. Atala A, Cima LG, Kim W, Paige KT, Vacanti JP, Retik AB, et al. Injectable alginate seeded with chondrocytes as a potential treatment for vesicoureteral reflux. *J Urol*. 1993;150:745–7.
6. Westhaus E, Messersmith PB. Triggered release of calcium from lipid vesicles: a bioinspired strategy for rapid gelation of polysaccharide and protein hydrogels. *Biomaterials*. 2001;22:453–62.
7. Gulrez S, Al-Assaf S, Phillips G. Hydrogels: methods of preparation, characterisation and applications. In: Carpi A, editor. *Progress in molecular and environmental bioengineering - from analysis and modeling to technology applications*. In Tech; 2011. p. 117–50.
8. Wu Y, Guo B, Ma PX. Injectable electroactive hydrogels formed via host–guest interactions. *ACS Macro Lett*. 2014;3:1145–50.
9. Ma X, Zhao Y. Biomedical applications of supramolecular systems based on host–guest interactions. *Chem Rev*. 2015;115:7794–839.
10. Slaughter BV, Khurshid SS, Fisher OZ, Khademhosseini A, Peppas NA. Hydrogels in regenerative medicine. *Adv Mater*. 2009;21:3307–29.
11. Kondiah PJ, Choonara YE, Kondiah PP, Marimuthu T, Kumar P, du Toit LC, et al. A review of injectable polymeric hydrogel systems for application in bone tissue engineering. *Molecules*. 2016;21:E1580.
12. Deng S, Li X, Yang W, He K, Ye X. Injectable in situ cross-linking hyaluronic acid/carboxymethyl cellulose based hydrogels for drug release. *J Biomater Sci Polym Ed*. 2018;29:1643–55.
13. Lu M, Liu Y, Huang YC, Huang CJ, Tsai WB. Fabrication of photo-crosslinkable glycol chitosan hydrogel as a tissue adhesive. *Carbohydr Polym*. 2018;181:668–74.
14. Portnov T, Shulimzon TR, Zilberman M. Injectable hydrogel-based scaffolds for tissue engineering applications. *Rev Chem Eng*. 2017;33:91–107.
15. Hozumi T, Kageyama T, Ohta S, Fukuda J, Ito T. Injectable hydrogel with slow degradability composed of gelatin and hyaluronic acid cross-linked by Schiff's base formation. *Biomacromolecules*. 2018;19:288–97.
16. Liao J, Jia Y, Wang B, Shi K, Qian Z. Injectable hybrid poly(ϵ -caprolactone)-b-poly(ethylene glycol)-b-poly(ϵ -caprolactone) porous microspheres/alginate hydrogel cross-linked by calcium gluconate crystals deposited in the pores of microspheres improved skin wound healing. *ACS Biomater Sci Eng*. 2018;4:1029–36.
17. Liu M, Zeng X, Ma C, Yi H, Ali Z, Mou X, et al. Injectable hydrogels for cartilage and bone tissue engineering. *Bone Res*. 2017;5:17014.
18. Jain S, Sandhu PS, Malvi R, Gupta B. Cellulose derivatives as thermoresponsive polymer: an overview. *J Appl Pharm Sci*. 2013;3:139–44.
19. Goes MF, Sinhorette MA, Consani S, Silva MA. Morphological effect of the type, concentration and etching time of acid solutions on enamel and dentin surfaces. *Braz Dent J*. 1998;9:3–10.
20. Pillai CKS, Paul W, Sharma CP. Chitin and chitosan polymers: chemistry, solubility and fiber formation. *Prog Polym Sci*. 2009;34:641–78.

21. Chen YH, Chung YC, Wang IJ, Young TH. Control of cell attachment on pH-responsive chitosan surface by precise adjustment of medium pH. *Biomaterials*. 2012;33:1336–42.
22. Weng L, Le HC, Talaie R, Golzarian J. Bioresorbable hydrogel microspheres for transcatheter embolization: preparation and in vitro evaluation. *J Vasc Interv Radiol*. 2011;22:1464–1470.e2.
23. Zhang W, Jin X, Li H, Zhang RR, Wu CW. Injectable and body temperature sensitive hydrogels based on chitosan and hyaluronic acid for pH sensitive drug release. *Carbohydr Polym*. 2018;186:82–90.
24. Parenteau-Bareil R, Gauvin R, Berthod F. Collagen-based biomaterials for tissue engineering applications. *Materials (Basel)*. 2010;3:1863–87.
25. Latifi N, Asgari M, Vali H, Mongeau L. A tissue-mimetic nanofibrillar hybrid injectable hydrogel for potential soft tissue engineering applications. *Sci Rep*. 2018;8:1047.
26. Kawase M, Michibayashi N, Nakashima Y, Kurikawa N, Yagi K, Mizoguchi T. Application of glutaraldehyde-crosslinked chitosan as a scaffold for hepatocyte attachment. *Biol Pharm Bull*. 1997;20:708–10.
27. Noah EM, Chen J, Jiao X, Heschel I, Pallua N. Impact of sterilization on the porous design and cell behavior in collagen sponges prepared for tissue engineering. *Biomaterials*. 2002;23:2855–61.
28. Geng X, Mo X, Fan L, Yin A, Fang J. Hierarchically designed injectable hydrogel from oxidized dextran, amino gelatin and 4-arm poly(ethylene glycol)-acrylate for tissue engineering application. *J Mater Chem*. 2012;22:25130–9.
29. Payne RG, McGonigle JS, Yaszemski MJ, Yasko AW, Mikos AG. Development of an injectable, in situ crosslinkable, degradable polymeric carrier for osteogenic cell populations. Part 2. Viability of encapsulated marrow stromal osteoblasts cultured on crosslinking poly(propylene fumarate). *Biomaterials*. 2002;23:4373–80.
30. Burdick JA, Prestwich GD. Hyaluronic acid hydrogels for biomedical applications. *Adv Mater*. 2011;23:H41–56.
31. Ma X, Xu T, Chen W, Qin H, Chi B, Ye Z. Injectable hydrogels based on the hyaluronic acid and poly (γ -glutamic acid) for controlled protein delivery. *Carbohydr Polym*. 2018;179:100–9.
32. S V, A S, Annapoorna M, R J, Subramania I, Shantikumar V N, et al. Injectable deferoxamine nanoparticles loaded chitosan-hyaluronic acid coacervate hydrogel for therapeutic angiogenesis. *Colloids Surf B Biointerfaces*. 2018;161:129–38.
33. Han Y, Li Y, Zeng Q, Li H, Peng J, Xu Y, et al. Injectable bioactive akermanite/alginate composite hydrogels for in situ skin tissue engineering. *J Mater Chem B*. 2017;5:3315–26.
34. Chan G, Mooney DJ. Ca^{2+} released from calcium alginate gels can promote inflammatory responses in vitro and in vivo. *Acta Biomater*. 2013;9:9281–91.
35. Mumcuoglu D, Fahmy-Garcia S, Ridwan Y, Nicke J, Farrell E, Kluijtmans SG, et al. Injectable BMP-2 delivery system based on collagen-derived microspheres and alginate induced bone formation in a time-and dose-dependent manner. *Eur Cell Mater*. 2018;35:242–54.
36. Wang K, Han Z. Injectable hydrogels for ophthalmic applications. *J Control Release*. 2017;268:212–24.
37. i-FACTOR™ Peptide enhanced bone graft, Westminster, Colorado USA. 2015. https://www.accessdata.fda.gov/cdrh_docs/pdf14/p140019d.pdf. Accessed 3 Dec 2015.
38. Prathamesh MK, April MK. Injectable hydrogels for cell delivery and tissue regeneration. <https://www.sigmaaldrich.com/technical-documents/articles/materials-science/injectable-hydrogels.html>. Accessed 1 Apr 2018.
39. Hasan A, Khattab A, Islam MA, Hweij KA, Zeitouny J, Waters R, et al. Injectable hydrogels for cardiac tissue repair after myocardial infarction. *Adv Sci (Weinh)*. 2015;2:1500122.
40. Bidarra SJ, Barrias CC, Granja PL. Injectable alginate hydrogels for cell delivery in tissue engineering. *Acta Biomater*. 2014;10:1646–62.
41. Shalini V, Sarah B, Ho-Man K, Hicham D, David W, Lakshmi S. Evaluation of enzymatically crosslinked injectable glycol chitosan hydrogel. *J Mater Chem B*. 2015;3:5511–22.
42. Sealant P. CoSeal surgical sealant (CoSeal) 2011. www.accessdata.fda.gov/cdrh_docs/pdf/p010022b.pdf. Accessed 14 Dec 2001.
43. Blake GM, Park-Holohan SJ, Cook GJ, Fogelman I. Quantitative studies of bone with the use of ^{18}F -fluoride and $^{99\text{m}}\text{Tc}$ -methylene diphosphonate. *Semin Nucl Med*. 2001;31:28–49.
44. Xu H, Othman SF, Magin RL. Monitoring tissue engineering using magnetic resonance imaging. *J Biosci Bioeng*. 2008;106:515–27.
45. Bakker MH, Tseng CCS, Keizer HM, Seevinck PR, Janssen HM, Van Slochteren FJ, et al. MRI visualization of injectable ureidopyrimidinone hydrogelators by supramolecular contrast agent labeling. *Adv Healthc Mater*. 2018;7:1701139.
46. Gudur M, Rao RR, Hsiao Y-S, Peterson AW, Deng CX, Stegmann JP. Noninvasive, quantitative, spatiotemporal characterization of mineralization in three-dimensional collagen hydrogels using high-resolution spectral ultrasound imaging. *Tissue Eng Part C Methods*. 2012;18:935–46.
47. Chakravarty R, Hong H, Cai W. Positron emission tomography image-guided drug delivery: current status and future perspectives. *Mol Pharm*. 2014;11:3777–97.
48. Lock LL, Li Y, Mao X, Chen H, Staedtke V, Bai R, et al. One-component supramolecular filament hydrogels as theranostic label-free magnetic resonance imaging agents. *ACS Nano*. 2017;11:797–805.
49. Ketcham R. X-ray Computer Tomography (CT) 2007. https://serc.carleton.edu/research_education/geochemsheets/techniques/CT.html. Accessed 6 Jun 2018.
50. Weissleder R. Scaling down imaging: molecular mapping of cancer in mice. *Nat Rev Cancer*. 2002;2:11–8.
51. Lei K, Ma Q, Yu L, Ding J. Functional biomedical hydrogels for in vivo imaging. *J Mater Chem B*. 2016;4:7793–812.
52. Tan J, Fu X, Sun CG, Liu C, Zhang XH, Cui YY, et al. A single CT-guided percutaneous intraosseous injection of thermosensitive simvastatin/poloxamer 407 hydrogel enhances vertebral bone formation in ovariectomized minipigs. *Osteoporos Int*. 2016;27:757–67.
53. Sivashanmugam A, Charoenlarp P, Deepthi S, Rajendran A, Nair SV, Iseki S, et al. Injectable shear-thinning CaSO_4 /FGF-18-incorporated Chitin-PLGA hydrogel enhances bone regeneration in mice cranial bone defect model. *ACS Appl Mater Interfaces*. 2017;9:42639–52.
54. Piert M, Zittel TT, Becker GA, Jahn M, Stahlschmidt A, Maier G, et al. Assessment of porcine bone metabolism by dynamic [^{18}F]fluoride ion PET: correlation with bone histomorphometry. *J Nucl Med*. 2001;42:1091–100.
55. Phelps ME, Chatzioannou A, Cherry S, Gambhir S. Molecular imaging of biological processes from microPET in mice to PET in patients. *Proc IEEE Int Symp Biomed Imaging*. 2002;1–9.
56. Tondera C, Hauser S, Krüger-Genge A, Jung F, Neffe AT, Lendlein A, et al. Gelatin-based hydrogel degradation and tissue interaction in vivo: insights from multimodal preclinical imaging in immunocompetent nude mice. *Theranostics*. 2016;6:2114–28.
57. Talukdar Y, Avti P, Sun J, Sitharaman B. Multimodal ultrasound-photoacoustic imaging of tissue engineering scaffolds and blood oxygen saturation in and around the scaffolds. *Tissue Eng Part C Methods*. 2014;20:440–9.
58. Yu J, Takanari K, Hong Y, Lee KW, Amoroso NJ, Wang Y, et al. Non-invasive characterization of polyurethane-based tissue

- constructs in a rat abdominal repair model using high frequency ultrasound elasticity imaging. *Biomaterials*. 2013;34:2701–9.
59. Chen Y, Li S, Li X, Zhang Y, Huang Z, Feng Q, et al. Non-invasive evaluation of injectable chitosan/nano-hydroxyapatite/collagen scaffold via ultrasound. *J Nanomater*. 2012;939821:7.
60. Leferink AM, van Blitterswijk CA, Moroni L. Methods of monitoring cell fate and tissue growth in three-dimensional scaffold-based strategies for *in vitro* tissue engineering. *Tissue Eng Part B Rev*. 2016;22:265–83.
61. McRobbie DW, Moore EA, Graves MJ, Prince MR. MRI from picture to proton. New York: Cambridge University Press; 2006. p. 30–42.
62. Kotecha M, Klatt D, Magin RL. Monitoring cartilage tissue engineering using magnetic resonance spectroscopy, imaging, and elastography. *Tissue Eng Part B Rev*. 2013;19:470–84.
63. Xu J, Chen Y, Yue Y, Sun J, Cui L. Reconstruction of epidural fat with engineered adipose tissue from adipose derived stem cells and PLGA in the rabbit dorsal laminectomy model. *Biomaterials*. 2012;33:6965–73.
64. Beaumont M, DuVal MG, Loai Y, Farhat WA, Sándor GK, Cheng HLM. Monitoring angiogenesis in soft-tissue engineered constructs for calvarium bone regeneration: an *in vivo* longitudinal DCE-MRI study. *NMR Biomed*. 2010;23:48–55.
65. Bible E, Dell'Acqua F, Solanky B, Balducci A, Crapo PM, Badylak SF, et al. Non-invasive imaging of transplanted human neural stem cells and ECM scaffold remodeling in the stroke-damaged rat brain by ^{19}F - and diffusion-MRI. *Biomaterials*. 2012;33:2858–71.
66. Hsueh Y-S, Chen Y-S, Tai H-C, Mestak O, Chao S-C, Chen Y-Y, et al. Laminin-alginate beads as preadipocyte carriers to enhance adipogenesis *in vitro* and *in vivo*. *Tissue Eng Part A*. 2017;23:185–94.
67. Roeder E, Henrionnet C, Goebel JC, Gambier N, Beuf O, Grenier D, et al. Dose-response of superparamagnetic iron oxide labeling on mesenchymal stem cells chondrogenic differentiation: a multi-scale *in vitro* study. *PLoS ONE*. 2014;9:e98451.
68. Mertens ME, Frese J, Bölükbas DA, Hrdlicka L, Golombek S, Koch S, et al. FMN-coated fluorescent USPIO for cell labeling and non-invasive MR imaging in tissue engineering. *Theranostics*. 2014;4:1002–13.
69. Dittmar R, Potier E, van Zandvoort M, Ito K. Assessment of cell viability in three-dimensional scaffolds using cellular auto-fluorescence. *Tissue Eng Part C Methods*. 2012;18:198–204.
70. Pan D, Pramanik M, Senpan A, Allen JS, Zhang H, Wickline SA, et al. Molecular photoacoustic imaging of angiogenesis with integrin-targeted gold nanobeacons. *FASEB J*. 2011;25:875–82.
71. Cai X, Zhang YS, Xia Y, Wang LV. Photoacoustic microscopy in tissue engineering. *Mater Today*. 2013;16:67–77.
72. Liang X, Graf BW, Boppart SA. Imaging engineered tissues using structural and functional optical coherence tomography. *J Biophotonics*. 2009;2:643–55.
73. Tondera C, Wieduwild R, Röder E, Werner C, Zhang Y, Pietzsch J. *In vivo* examination of an injectable hydrogel system cross-linked by peptide-oligosaccharide interaction in immunocompetent nude mice. *Adv Funct Mater*. 2017;27:1605189.